

1 **Assessing the consistency between short-term global temperature trends in**  
2 **observations and climate model projections**

3

4 Patrick J. Michaels  
5 George Mason University  
6 Fairfax, Virginia  
7 pmichaels@cato.org

8

9 Paul C. Knappenberger  
10 New Hope Environmental Services, Inc.  
11 Charlottesville, Virginia  
12 chip@nhes.com

13

14 John R. Christy  
15 Earth System Science Center, NSSTC  
16 University of Alabama in Huntsville  
17 Huntsville, Alabama  
18 john.christy@nsstc.uah.edu

19

20 Chad S. Herman  
21 Manalapan, New Jersey  
22 chad.herman.us@gmail.com

23

24 Lucia M. Liljegren  
25 Lisle, Illinois  
26 lucia@rankexploits.com

27

28 James D. Annan  
29 Research Institute for Global Change  
30 Yokohama, Japan  
31 jdannan@jamstec.go.jp

32 **Abstract**

33

34 Assessing the consistency between short-term global temperature trends in observations  
35 and climate model projections is a challenging problem. While climate models capture  
36 many processes governing short-term climate fluctuations, they are not expected to  
37 simulate the specific timing of these somewhat random phenomena—the occurrence of  
38 which may impact the realized trend. Therefore, to assess model performance, we  
39 develop distributions of projected temperature trends from a collection of climate models  
40 running the IPCC A1B emissions scenario. We evaluate where observed trends of length  
41 5 to 15 years fall within the distribution of model trends of the same length. We find that  
42 current trends lie near the lower limits of the model distributions, with cumulative  
43 probability-of-occurrence values typically between 5% and 20%, and probabilities below  
44 5% not uncommon. Our results indicate cause for concern regarding the consistency  
45 between climate model projections and observed climate behavior under conditions of  
46 increasing anthropogenic greenhouse-gas emissions.

47

48 **1. Background**

49

50 While global warming is often described as accelerating, in fact, the rate of increase in  
51 global average surface temperatures has slowed in recent years. However, the  
52 significance of this slowdown has not been well-established as most discussions about the  
53 issue lack sufficient grounding in the full distribution of the expectations to which the  
54 observations are being compared. Recent research has begun to focus on this issue, but

55 has only done so in a limited scope. *Easterling and Wehner* [2009] determined the  
56 probability distribution for projected trends from a collection of climate models, but  
57 limited their analysis to trends of 10 years in length, while *Knight et al.* [2009] looked at  
58 the projected ranges for a variety of trend lengths, but from only one climate model.

59

60 Here we extend the results of previous analyses to determine the probability distribution  
61 of short-period trends in global temperature (in length from 5 to 15 years) as projected by  
62 a collection of climate models run under the Intergovernmental Panel on Climate Change  
63 (IPCC) A1B (“business-as-usual”) emissions scenario. We then evaluate where the  
64 current values of the observed trends of similar length fall within the model distributions.

65

## 66 **2. Data and Methods**

67

### 68 *2.1 Climate Model Projections*

69

70 Monthly output from 20 climate models (51 model runs) incorporated in the IPCC *Fourth*  
71 *Assessment Report* [2007] run under the IPCC’s A1B emissions scenario [*Nakićenović*  
72 *and Swart, 2000*] was obtained from Coupled Model Intercomparison Project 3 (CMIP3)  
73 [*Meehl et al., 2007*] database archived at the Program for Climate Model Diagnosis and  
74 Intercomparison (PCMDI) at the Lawrence Livermore National Laboratory. From these  
75 model projections, monthly global-average anomalies of surface and lower troposphere  
76 temperature were developed (see Auxiliary Material).

77

78 The model average temperature trend is very consistent for all trend lengths within the  
79 first two decades of the 21<sup>st</sup> century but begins to increase in the decades immediately  
80 thereafter. We therefore limit our analysis to the period January 2001 through December  
81 2020 and consider this period to represent the expected behavior of the observed global  
82 average temperature during the first two decades of the 21<sup>st</sup> century.

83

84 Since the model runs contain internal (random) climate variability in addition to a  
85 response to the prescribed changes in radiative forcing, trends in model projections  
86 cannot be expected to match trends in observations over relatively short time spans—a  
87 few years to a decade or two. However, climate models do capture many characteristics  
88 of the primary processes driving short-term variability [*IPCC*, 2007, Chapter 8].  
89 Therefore, the distribution of short-term temperature trends (of all lengths) from model  
90 projections should with high probability encompass the trends (of similar length) in the  
91 observed data if the model projections are accurately capturing climate behavior. While  
92 the observed trend falling within the model distribution of trends is not conclusive proof  
93 of the validity of climate model projections, it does serve as a necessary condition.

94

95 We develop the distributions of projected short-term temperature trends both for the  
96 surface and the lower troposphere. Through each individual model run, we calculate the  
97 moving linear trends through the first 20 years of monthly projections for time periods  
98 with lengths ranging from 5 years (60 months) to 15 years (180 months). For each model  
99 run, we develop the set of all available trends of each length. For example, for 5-year  
100 trends, we calculate the trend for the period January 2001-December 2005, February

101 2001-January 2006, March 2001-February 2006, successively stepping one month at a  
102 time thorough all 60-month periods and ending with January 2016-December 2020. The  
103 total number of trends determined from each model run declines with the increasing trend  
104 length, from 180 5-year trends, to 60 15-year trends. For each trend length, we then  
105 combine the set of trends calculated from each of the 51 model runs—weighted to  
106 produce an equal contribution from each climate model (regardless of the number of  
107 available runs)—into a single distribution representing a sample of the overall population  
108 of potential realities contained in the collection of climate models [*Annan and*  
109 *Hargreaves*, 2010]. Weighting each model run equally does not materially affect our  
110 results. The distribution of 5-yr trends contains contributions from 9,180 (180 x 51)  
111 elements, a number which declines to 3,060 for 15-yr trends (60 x 51). However, all  
112 individual elements are not independent of each other as the moving trends within a  
113 single model run are to some degree correlated.

114

## 115 *2.2 Observed Temperature Record*

116

117 We use observed records of global average surface temperature anomalies compiled  
118 monthly by the Climate Research Unit of the University of East Anglia and the Hadley  
119 Centre (HadCRU) [*Brohan et al.*, 2006], by the Goddard Institute for Space Studies  
120 (GISS) [*Hansen et al.*, 2006] and by the National Climatic Data Center (NCDC) [*Smith et*  
121 *al.*, 2008]. Additionally we use observed records of global average lower troposphere  
122 temperatures measured by Microwave Sounder Units (MSU) aboard satellites as

123 complied by the University of Alabama-Huntsville (UAH) [*Christy et al.*, 2003] and by  
124 Remote Sensing Systems (RSS) [*Mears and Wentz*, 2009].

125

126 From the observed global temperature anomalies in each dataset, we calculate the linear  
127 trends using simple least squares regression of lengths 5 years (60 months) to 15 years  
128 (180 months) ending with the most recent data available (December 2009) (see Auxiliary  
129 Table 1 for the observed trend values).

130

131 Observed trends of length greater than 9 years include data from a period of time prior to  
132 the IPCC AR4 climate model projections (which generally begin in January 2001).  
133 However, the rate of increase of radiative forcing from anthropogenic emissions changes  
134 very little between the mid-1990s and the first few decades of the 21<sup>st</sup> century under the  
135 A1B emissions scenario [*IPCC*, 2007] so a comparison between observed behavior over  
136 the past 15 years and the model expected behavior during the period 2001-2020 is  
137 appropriate. We do not extend our analysis into trends of length greater than 15 years as  
138 the observed trend begins to be influenced by the 1991 eruption of Mt. Pinatubo—a type  
139 of natural forcing not included in the A1B emissions scenario.

140

### 141 **3. Results and Discussion**

142

143 There are several options to assess the cumulative probability of a particular trend value  
144 within the model distributions of projected trends. For instance, the cumulative  
145 probability of a 10-yr trend in global average surface temperatures with a value less than

146 or equal to zero can be determined directly from the elements of the distribution of model  
147 projected 10-yr trends by using ranked percentiles (which yields a cumulative probability  
148 of 6.3%), by using Student's t-distribution conservatively with 31 degrees of freedom  
149 representing the weighted combination of the 51 model runs (which yields a cumulative  
150 probability of 8.4%), or by fitting a normal distribution (which yields a cumulative  
151 probability of 7.9%). The results of these three solutions are very similar across all trend  
152 lengths, indicating that the determination of the cumulative probability is not overly  
153 sensitive to the choice of method. As such, subsequently we will only report the results  
154 using the assumption of normality.

155

156 These results in the previous example can be compared with other assessments of model  
157 trend probabilities. *Easterling and Wehner* [2009] used a similar statistical methodology,  
158 but used model projections from the SRES A2 scenario to determine the probability of a  
159 10-yr trend less than or equal to zero. They reported a probability of “about 10%” for  
160 such an occurrence during the first half of the 21<sup>st</sup> century. This value is slightly greater  
161 than the value from our methodology, mostly likely, because the A2 scenario examined  
162 by *Easterling and Wehner* [2009] includes less forcing during the first half of the 21<sup>st</sup>  
163 century than does the A1B scenario we used. *Knight et al.* [2009] examined variability  
164 within the trends produced by the HadCM3 climate model when run under a variety of  
165 emissions scenarios and model settings. *Knight et al.* [2009] found that a 10-yr trend falls  
166 just inside the 90% range of trends produced by the HadCM3 model—a value apparently  
167 similar to ours.

168

169 In Figure 1 we present a general depiction of the model probability distributions for  
170 trends of length 5 to 15 years for surface temperatures. As the length of the trend  
171 increases, the probably range tightens. This general solution can be used to assess the  
172 model-based probability of any and all short-term trends within the first 20 years of the  
173 21<sup>st</sup> century. For example, the probability of a trend in global average temperatures that is  
174 less than or equal to zero becomes 5% or less at a length of about 11 years (132 months).  
175 The probability distributions for the projected trends in the lower troposphere are very  
176 similar (see Auxiliary Figure 1). The average model projected trend in the lower  
177 troposphere is about 20% larger than the surface (0.025°C/yr vs. 0.020°C/yr) and the  
178 spread about the mean is slightly larger as well.

179

180 The spread of the distributions of model projected trends is governed both by statistical  
181 uncertainty about the best-fit linear trend that results from random variability that is  
182 independent from month-to-month, as well as by the influence of random (over the  
183 longer-term) low-frequency variability that is correlated over times scales of months to  
184 decades and which may alter the value of the short-term trends for an extended time  
185 period. Our working hypothesis is that these random processes operate to influence  
186 model trends to the same degree as they do observed trends. Therefore, we assume that  
187 the model trend distributions represent the spread of potential realities (including these  
188 uncertainties), of which the single realization of the observed trend is a member.

189

190 One notable exception to this assumption concerns the true observational errors, such as  
191 those arising from incomplete spatial coverage, station number changes, and non-



192 climatological influences on the temperature measurements. These errors do not occur in  
193 the model projections for which the temperature is precisely known. Estimates of the size  
194 of observational errors are available for each observed dataset and we incorporate them  
195 into Monte Carlo simulations to ascertain their influence on variability of trends ranging  
196 from 5 to 15 years in length. We add this variability to the variability in the model trend  
197 distributions (see Auxiliary Material). This results in a slight broadening of the  
198 distributions.

199

200 From these adjusted distributions, derived separately for the surface and the lower  
201 troposphere, we determine the cumulative probability of occurrence of the value of the  
202 observed trend (ending in December 2009) ranging in length from 5 to 15 years in each  
203 of the five observed datasets—three compilations of surface temperatures and two  
204 compilations of lower tropospheric temperatures (Figure 2).

205

206 The cumulative probabilities of the observed trend values typically are less than 20%  
207 (with the exception of GISS dataset). In all datasets the cumulative occurrence  
208 probability of the current 8-yr trend is about 10% or less, and in all datasets except the  
209 GISS dataset, there is less than a 10% probability of current values for trends of 7, 8, 9,  
210 12, and 13 years in length. The values for these same trend lengths from some datasets  
211 fall beneath the 5% cumulative probability indicating an expectation of occurrence of less  
212 than 1 in 20 (a typical measure of statistical significance). In general, the cumulative  
213 probabilities of the observed trends are lower for the lower troposphere than for the  
214 surface.

215

216 **4. Conclusions**

217

218 For most observational datasets of global average temperature, the trends from length 5 to  
219 15 years lie along the lower tails of the probability distributions from the collection of  
220 climate model projections under the SRES A1B emissions scenario. Typically the  
221 probability of occurrence of the observed trend values lies between 5% and 20%,  
222 depending on the dataset and the trend length. In the HadCRU, RSS, and UAH observed  
223 datasets, the current value of trends of length 8, 12, and 13 years is expected from the  
224 models to occur with a probability of less than 1 in 20. Taken together, our results raise  
225 concern about the consistency between the observed evolution of global temperatures in  
226 recent years and the climate model projections of that evolution.

227

228 Possible reasons for why current trends are unusual when set among model projections  
229 include unknown errors in the observational temperature record, differences in the true  
230 vs. A1B-defined anthropogenic forcing changes, insufficiencies of the climate models to  
231 accurately replicate the characteristics of natural variability, inaccuracies in climate  
232 model transient climate evolution, and the overestimation by climate models of the actual  
233 climate sensitivity. These are in addition to the possibility that current trends represent  
234 simply a rare but not impossible situation that is generally captured by the climate  
235 models.

236

237 As global emissions of carbon dioxide—the primary anthropogenic climate forcing  
238 agent—have been increasing during recent years at a rate similar to that specified in the  
239 A1B scenario [*Nakićenović and Swart, 2000; EIA, 2008*], it is unlikely that the difference  
240 between observed and projected trends arises from a significant underestimate of the  
241 changes in climate forcing prescribed by the A1B scenario. Similarly, while there are  
242 clearly differences among the observed trend values derived from the various  
243 observational datasets, all trends through the observed data fall in the lower tails of model  
244 projections, so it is unlikely that errors in the observations (which may include a warming  
245 bias in surface observations in recent years, [e.g., *McKittrick and Michaels, 2007;*  
246 *Klotzbach et al., 2009*] are the primary cause of the observed/projected differences. This  
247 leads to the conclusion that a large part of the differences between the observed trends  
248 and model-projected trends lies with the internal workings of the models. This conclusion  
249 is supported by results which indicate that natural variations in ocean/atmospheric  
250 circulation patterns are in part responsible for the recent slowdown in the rate of global  
251 temperature rise [*Keenlyside et al., 2008; Swanson and Tsonis, 2009*] and that  
252 inadequately-modeled decadal-scale variations in stratospheric water vapor have a  
253 significant influence on global temperature trends, including contributing to a reduced  
254 trend in recent years [*Solomon et al., 2010*]. Further, some results indicate that the model  
255 determinations of climate sensitivity may be too large [e.g., *Wyant et al., 2006; Spencer*  
256 *and Braswell, 2008*]. It can also be noted that the discrepancy between observed trends  
257 and projected trends is greater for satellite than surface observations.

258

259 Our results stand in contrast to results such as *Rahmstorf et al.* [2007] which concluded  
260 that observed trends through global average temperatures are increasing at a rate near the  
261 upper end of the IPCC projected range. The primary reasons for the contrasting  
262 conclusions are that our analysis is based upon updated climate model runs, more recent  
263 observed data, and a more comprehensive analysis of model projections.

264

## 265 **6. References**

266

267 Annan, J. D., and J. C. Hargreaves (2010), Reliability of the CMIP3 ensemble. *Geophys.*  
268 *Res. Lett.*, *37*, L02703, doi:10.1029/2009GL041994.

269

270 Brohan, P., J. J. Kennedy, I. Harris, S. F. B. Tett and P.D. Jones (2006), Uncertainty  
271 estimates in regional and global observed temperature changes: a new dataset from 1850,  
272 *J. Geophys. Res.*, *111*, D12106, doi:10.1029/2005JD006548.

273

274 Christy J. R., R. W. Spencer, W. B. Norris, W. D. Braswell, and D. E. Parker (2003),  
275 Error estimates of version 5.0 of MSU–AMSU bulk atmospheric temperatures. *J. Atmos.*  
276 *Oceanic Technol.*, *20*, 613–629.

277

278 Easterling, D. R., and M. F. Wehner (2009), Is the climate warming or cooling? *Geophys.*  
279 *Res. Lett.*, *36*, L08706, doi:10.1029/2009GL037810.

280

281 Energy Information Administration (EIA) (2008), *International Energy Annual, 2006*.  
282 U.S. Department of Energy, Washington, D.C.,  
283 <http://www.eia.doe.gov/pub/international/iealf/tableh1co2.xls>  
284  
285 Hansen, J., M. Sato, R. Ruedy, K. Lo, D. W. Lea and M. Medina-Elizade (2006), Global  
286 temperature change, *Proc. Natl. Acad. Sci.*, *103*, 14288-14293,  
287 doi:10.1073/pnas.0606291103.  
288  
289 Intergovernmental Panel on Climate Change (IPCC) (2007), *Climate Change 2007: The*  
290 *Physical Science Basis. Contribution of Working Group I to the Fourth Assessment*  
291 *Report of the Intergovernmental Panel on Climate Change*, edited by S. Solomon et al.,  
292 996 pp., Cambridge Univ. Press, Cambridge, U. K.  
293  
294 Keenlyside, N. S., M. Latif, J. Jungclaus, L. Kornblueh and E. Roeckner (2008),  
295 Advancing decadal-scale climate prediction in the North Atlantic sector. *Nature*, *453*, 84-  
296 88, doi:10.1038/nature06921.  
297  
298 Klotzbach, P. J., R. A. Pielke Sr., R. A. Pielke Jr., J. R. Christy, and R. T. McNider  
299 (2009), An alternative explanation for differential temperature trends at the surface and in  
300 the Lower Troposphere, *J. Geophys. Res.*, *114*, D21102, doi:10.1029/2009JD011841.  
301  
302 Knight, J., Kennedy, J. J., Folland, C., Harris, G., Jones, G. S., Palmer, M., Parker, D.,  
303 Scaife, A., & Stott, P. (2009), Do global temperature trends over the last decade falsify

304 climate predictions? In: Peterson, T. C., & Baringer, M.O. (eds), "State of the Climate in  
305 2008" Special Supplement to the *Bull. Am. Meteorol. Soc.*, 90-91.

306

307 McKittrick, R. R., and P. J. Michaels (2007), Quantifying the influence of anthropogenic  
308 surface processes inhomogeneities on gridded global climate data. *J. Geophys. Res.*, *112*,  
309 D24S09, doi:10.1029/2007JD008465.

310

311 Mears, C. A., and F. J. Wentz (2009), Construction of the RSS V3.2 lower tropospheric  
312 temperature dataset from the MSU and AMSU microwave sounders. *J. Atmos. Ocean.  
313 Tech.*, *26*, 1493-1509.

314

315 Meehl, G. A., et al. (2007), The WCRP CMIP3 multi-model dataset: A new  
316 era in climate change research, *Bull. Am. Meteorol. Soc.*, *88*, 1383-1394.

317

318 Nakićenović, N., and R. Swart (2000), *Intergovernmental Panel on Climate Change  
319 Special Report on Emissions Scenarios*, Cambridge Univ. Press, Cambridge, U. K.

320

321 Rahmsdorf, S., A. Cazenave, J. A. Church, J. E. Hansen, R. F. Keeling, D. E. Parker, and  
322 R. C. Somerville (2007), Recent climate observations compared to projections. *Science*,  
323 *316*, 709.

324

325 Smith, T.M., R. W. Reynolds, T. C. Peterson, and J. Lawrimore (2008), Improvements to  
326 NOAA's historical merged land-ocean surface temperature analysis (1880-2006), *J.*  
327 *Clim.*, *21*, 2283-2296.

328

329 Solomon, S., K. H. Rosenlof, R. W. Portmann, J. S. Daniel, S. M. Davis, T. J. Sanford,  
330 and G-K Plattner (2010), Contributions of stratospheric water vapor to decadal changes  
331 in the rate of global warming, *Science*, *327*, 1219-1223.

332

333 Spencer, R. W., and W. D. Braswell (2008), Potential biases in feedback diagnosis from  
334 observations data: a simple model demonstration, *J. Clim.*, *21*, 5624-5628.

335

336 Swanson, K. L. and A. A. Tsonis (2009), Has the climate recently shifted? *Geophys. Res.*  
337 *Lett.*, *36*, L06711, doi:10.1029/2008GL037022.

338

339 Wyant, M. C., M., Khairoutdinov, and C. S. Bretherton (2006), Climate sensitivity and  
340 cloud response of a GCM with a superparameterization. *Geophys. Res. Lett.*, *33*, L06714.

341

342 **Figure Captions**

343

344 Figure 1. Cumulative probability distribution of trend values for trends ranging in length  
345 from 5 to 15 years derived from 20 models under SRES A1B for the period January 2001  
346 through December 2020 for global average surface temperatures. The 95% confidence  
347 range is shaded in grey and a zero trend is indicated by the horizontal black line.

348

349

350 Figure 2. Cumulative probabilities of the current observed values of the trends ranging in  
351 length from 5 to 15 years (each ending in December 2009) through average global  
352 surface temperature anomalies and lower troposphere temperature anomalies as compiled  
353 within five observed temperature datasets.

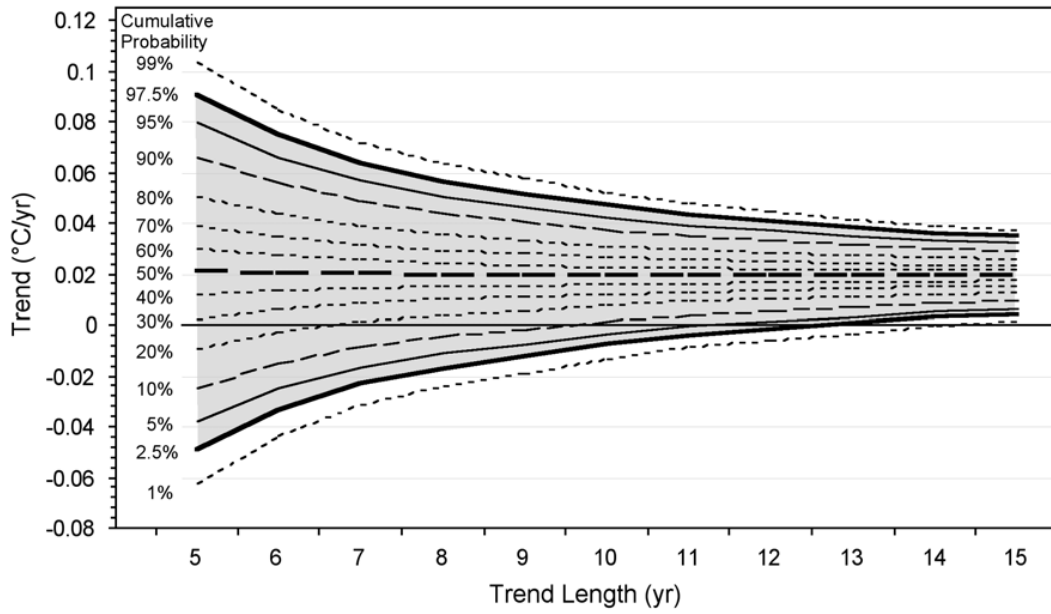
354

355



356 Figure 1.

357



358

359

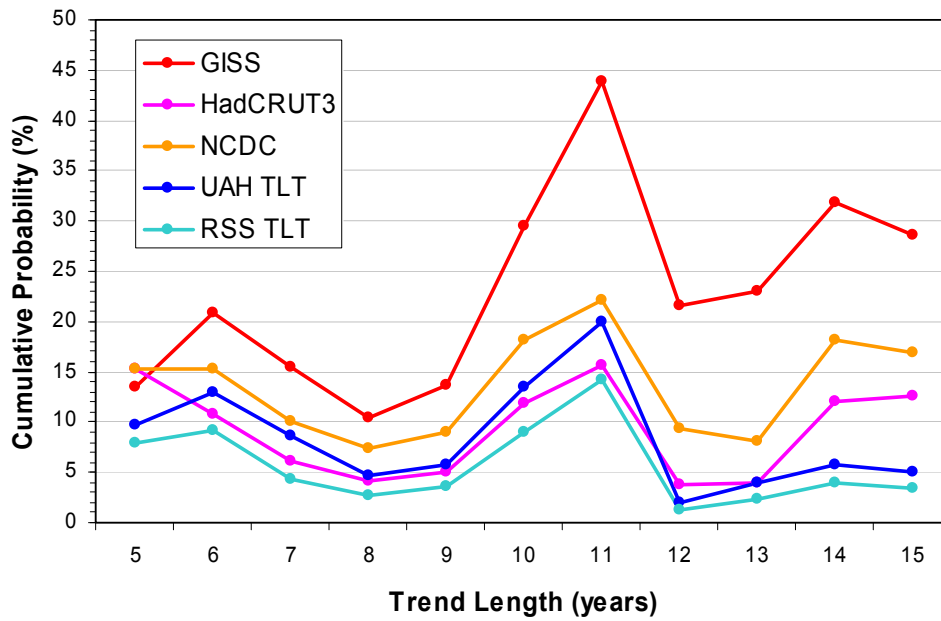
360 Figure 1. Cumulative probability distribution of trend values for trends ranging in length  
361 from 5 to 15 years derived from 20 models under SRES A1B for the period January 2001  
362 through December 2020 for global average surface temperatures. The 95% confidence  
363 range is shaded in grey and a zero trend is indicated by the horizontal black line.

364 Figure 2.

365

366

367



368

369 Figure 2. Cumulative probabilities of the current observed values of the trends ranging in  
370 length from 5 to 15 years (each ending in December 2009) through average global  
371 surface temperature anomalies and lower troposphere temperature anomalies as compiled  
372 within five observed temperature datasets.

373

374

375

376

1 **Auxiliary material for paper ...**

2

3

4 **Assessing the consistency between short-term global temperature trends in**

5 **observations and climate model projections**

6

7 Patrick J. Michaels  
8 George Mason University  
9 4400 University Drive, Fairfax, Virginia 22030  
10 pmichaels@cato.org

11

12 Paul C. Knappenberger  
13 New Hope Environmental Services, Inc.  
14 536 Pantops Center, #402  
15 Charlottesville, Virginia 22911  
16 chip@nhes.com

17

18 John R. Christy  
19 Earth System Science Center, NSSTC  
20 University of Alabama in Huntsville  
21 Huntsville, Virginia 35805  
22 john.christy@nsstc.uah.edu

23

24 Chad S. Herman  
25 Marlboro, New Jersey  
26 chad.herman.us@gmail.com

27

28 Lucia M. Liljegren  
29 Lisle, Illinois  
30 lucia@rankexploits.com

31

32 James D. Annan  
33 Research Institute for Global Change  
34 Yokohama, Japan  
35 jdannan@jamstec.go.jp

36

37

38

39 *Auxiliary Methods*

40

41 *1. Climate Model Selection*

42 Gridded monthly projections of surface and atmospheric air temperatures from 51  
43 individual climate model runs representing 20 separate climate models were downloaded  
44 from the PCMDI CMIP3 model archive database. Model selection consisted of only  
45 those listed in IPCC AR4 Table 10.4. and runs whose 20C3M runs continue forward with  
46 SRES A1B. Of these models, two had to be eliminated. There was no atmospheric  
47 temperature data available for MIUB ECHO-G so lower troposphere temperatures could  
48 not be simulated. CNRM CM 3 was eliminated because the netCDF files did not  
49 represent the atmospheric temperature on a consistent set of pressure levels.

50

51 The models and the numbers of runs we used in our analysis are included in Table 1  
52 (details of these climate models can be found at the PCMDI archive, [http://www-  
53 pcmdi.llnl.gov/ipcc/model\\_documentation/ipcc\\_model\\_documentation.php](http://www-pcmdi.llnl.gov/ipcc/model_documentation/ipcc_model_documentation.php)).

54

55 Table 1. Model names and number of available runs.

56

<b>Model Name</b>	<b>Number of Runs</b>
BCCR BCM 2.0	1
CCCMA CGCM 3.1 T47	5
CCCMA CGCM 3.1 T63	1
CSIRO MK 3.0	1
ECHAM5/MPI-OM	4
GFDL CM 2.0	1
GFDL CM 2.1	1
GISS AOM	2
GISS EH	3
GISS ER	5
IAP FGOALS 1.0g	3

INM CM 3.0	1
IPSL CM 4	1
MIROC 3.2 HIRES	1
MIROC 3.2 MEDRES	3
MRI CGCM 2.3.2a	5
NCAR CCSM 3.0	7
NCAR PCM 1	4
UKMO HAD CM 3	1
UKMO HADGEM 1	1

57

58

59 ***2. Creation of monthly surface air temperature anomalies***

60 For each model run, the projected monthly gridded surface air temperature values were  
61 spatially averaged to produce global average temperatures for each month. The global  
62 average monthly temperatures were then converted to global average monthly  
63 temperature anomalies by subtracting the climatology for each model run over the period  
64 January 2001 through December 2020.

65

66 ***3. Creation of monthly synthetic MSU lower troposphere temperatures anomalies***

67 Microwave Sounder Units (MSU) carried aboard a series of NASA satellites monitor  
68 bulk average temperatures in the atmosphere. A temperature for the lower troposphere  
69 can be generated from the MSU observations by a weighted combination of several MSU  
70 frequency channels. To properly compare the observed MSU lower troposphere  
71 temperatures with climate model projections, model-generated atmosphere temperature  
72 data must be used to develop an equivalent synthetic MSU lower troposphere temperature  
73 product. To this end, we employed the procedure described by Santer et al. [1999] as  
74 implemented by Santer and Doutriaux [2005] as part of the PCMDI Climate Data  
75 Analysis Tools package to produce gridded monthly, synthetic MSU lower troposphere

76 temperatures from each model run. The gridded temperature values were spatially  
77 averaged to produce global average temperatures for each month. The global average  
78 monthly temperatures were then converted to global average monthly temperature  
79 anomalies by subtracting the climatology for each model run over the period January  
80 2001 through December 2020.

81

## 82 *References*

83

84 Santer, B., and C. Doutriaux, 2005. Subroutine MSUWEIGHTS3.f, Part of the Climate  
85 Data Analysis Tools available from the Lawrence Livermore National Laboratory's  
86 (LLNL) Program for Climate Model Diagnosis and Intercomparison (PCMDI),  
87 [http://www2pcmdi.llnl.gov/svn/repository/cdat/tags/CDAT4.3/contrib/MSU/Src/msuwei](http://www2pcmdi.llnl.gov/svn/repository/cdat/tags/CDAT4.3/contrib/MSU/Src/msuweight.f)  
88 [ght.f](http://www2pcmdi.llnl.gov/svn/repository/cdat/tags/CDAT4.3/contrib/MSU/Src/msuweight.f) and archived at <http://www.webcitation.org/5owusvk91>.

89

90

91

92 Santer, B. D., J. J. Hnilo, T. M. L. Wigley, J. S. Boyle, C. Doutriaux, M. Fiorino, D. E.  
93 Parker, and K. E. Taylor (1999), Uncertainties in observationally based estimates of  
94 temperature change in the free atmosphere, *J. Geophys. Res.*, 104(D6), 6305–6333.

95

## 96 *4. Accounting for “observational error”*

97 Observations of the average global temperature contain uncertainties that model projected  
98 temperatures do not. These “observational errors” include such things as incomplete  
99 spatial coverage, changing number of stations within gridcells, changing observational

100 practices, etc. The magnitude of these errors has been quantified in the literature  
101 describing each of the observed datasets that we used in our study. For the UAH MSU  
102 lower troposphere temperatures, the standard errors for the monthly anomalies are given  
103 in Christy et al [2003]. Brohan et al. [2008] describes the monthly components of  
104 observational error that are contained in the HadCRUT3 surface temperatures. For the  
105 GISS [Hansen et al., 2006] and NCDC [Smith et al., 2008] surface temperatures,  
106 however, only the standard error of the annual anomalies are presented. The information  
107 quantifying the errors of monthly global anomalies in the RSS MSU lower troposphere  
108 temperatures was obtained through personal communications [Mears, 2010].

109

110 Since we are using monthly anomalies, we require estimates of the errors for monthly  
111 anomalies. The Hadley Center website  
112 (<http://hadobs.metoffice.com/hadcrut3/diagnostics/global/nh+sh/>) provides global  
113 temperature anomalies as well as error ranges for the HadCRUT3 dataset, for both  
114 monthly and annual anomalies. If the errors were independent from one another at the  
115 monthly timescale, the annual error would be equal to the monthly error divided by the  
116 square root of 12 (or by a factor of 3.46). However, comparing the listed monthly and  
117 annual error ranges, we find that the annual error in the HadCRUT3 is only reduced by a  
118 factor of 1.73 from the monthly errors (or the square root of 3), indicating that the errors  
119 are not independent (Table 2). The major source of observational error in the global  
120 temperature anomalies compiled in the HadCRUT3 data is a result of incomplete spatial  
121 coverage, with a minor contribution from bias [Brohan et al., 2008]. The error resulting

122 from bias has a lower-frequency variability than does the error from incomplete spatial  
 123 coverage [Brohan et al., 2008].  
 124  
 125 Since we have only estimates of the error of the annual global anomalies available from  
 126 the GISS [Hansen et al., 2006] and the NCDC [Smith et al., 2008] datasets, we will use  
 127 the HadCRUT monthly-to-annual scaling factor to guide our estimation of the error about  
 128 the monthly anomalies reported in the NCDC and GISS datasets. Smith et al. [2008]  
 129 finds that in the NCDC dataset, the contribution from bias is greater than the contribution  
 130 from incomplete spatial coverage, as they use interpolation to increase the spatial  
 131 coverage of the observations. Since bias error is more temporally correlated than error  
 132 resulting from incomplete spatial coverage, we reduce the scaling factor that we  
 133 determined from the HadCRUT3 data from 1.73 down to 1.50 for the NCDC dataset to  
 134 account for the likely reduced degrees of freedom in the NCDC error compared with  
 135 HadCRUT3 errors. As the characteristics of the spatial coverage of the GISS data are  
 136 similar to that of the NCDC data, we apply the 1.50 scaling factor to the GISS data as  
 137 well. The reported annual error, along with our estimated monthly error for these datasets  
 138 is listed in Table 2.

139

140 Table 2. The standard error of “observational errors” of the annual and monthly global  
 141 temperature anomalies from the 5 observed datasets used in our analysis.

142

143	<u>Dataset</u>	<u>Annual Error (°C)</u>	<u>Monthly Error (°C)</u>
144	HadCRUT3*	0.045	0.078
145	NCDC	0.03	0.045
146	GISS	0.025	0.0375
147	UAH MSU	0.075	0.10
148	RSS MSU	0.043	0.047

149



150 \*This is an average for the HadCRUT3 errors (over 1979-2009) as the actual errors are  
151 computed monthly and differ from month to month  
152

153 To assess the influence of these observational errors on the trends of length 5 to 15 years  
154 ending in December 2009 in each dataset, we used a Monte Carlo simulation, drawing  
155 each monthly data element randomly from a normal distribution with a mean equal to the  
156 observed monthly global temperature anomaly, and a standard deviation equal to the  
157 monthly error listed in Table 1 (for the HadCRUT3 data, we used the error explicitly as  
158 reported on the Hadley Center web site,  
159 <http://hadobs.metoffice.com/hadcrut3/diagnostics/global/nh+sh/>, which differs from  
160 month to month). We performed 10,000 replications for each series (from 5 to 15 years in  
161 length ending in December 2009) for each dataset, determining the linear least-squares  
162 trend through each. From the distributions of 10,000 values for each trend length for each  
163 dataset, we determined the standard deviation representing the trend variability due to  
164 observational errors assuming independence from month to month. The effect of  
165 correlations in the monthly errors was not assessed. The likelihood that the correlations in  
166 monthly errors vary considerably in time and across datasets makes it difficult to  
167 speculate whether the trend variability would be higher or lower than we determined  
168 assuming error independence on the specific 5 to 15 years trends in this study.  
169

170 We incorporated the influence of observational into our distributions of model trends by  
171 adding the standard deviation from observational error determined for each trend length  
172 and each observational dataset as described above, in quadrature to the standard deviation  
173 of the model trend distributions of the same length,  $\sigma_{x+y} = \sqrt{\sigma_x^2 + \sigma_y^2}$ , where  $\sigma_{x+y}$  is the

174 combined standard deviation,  $\sigma_x^2$  is the standard deviation of the model trend  
175 distributions, and  $\sigma_y^2$  is the standard deviation of observational error. Each distribution of  
176 modeled trends was broadened by the inclusion of the effect of observational errors.  
177  
178

179 Auxiliary Table 1. Value of the linear least-squares trend for lengths ranging from 5 years  
 180 (60 months) to 15 years (180 months) through global average temperature anomalies  
 181 ending in December 2009, from the five observed datasets used in this study.  
 182

Trend Length (yrs)	Trend (°C/yr)				
	GISS	HADCRUT3	NCDC	UAH MSU v5.2	RSS MSU v3.2
5	-0.01835	-0.01608	-0.01564	-0.03560	-0.04033
6	-0.00178	-0.01409	-0.00773	-0.01573	-0.02256
7	-0.00205	-0.01445	-0.00782	-0.01451	-0.02412
8	-0.00365	-0.01325	-0.00735	-0.01615	-0.02147
9	0.00169	-0.00761	-0.00242	-0.00797	-0.01232
10	0.01214	0.00292	0.00689	0.00542	0.00154
11	0.01783	0.00733	0.01037	0.01203	0.00882
12	0.01099	-0.00001	0.00511	-0.00283	-0.00522
13	0.01224	0.00226	0.00590	0.00395	0.00149
14	0.01556	0.00957	0.01189	0.00873	0.00715
15	0.01526	0.01061	0.01217	0.00937	0.00785

183

184

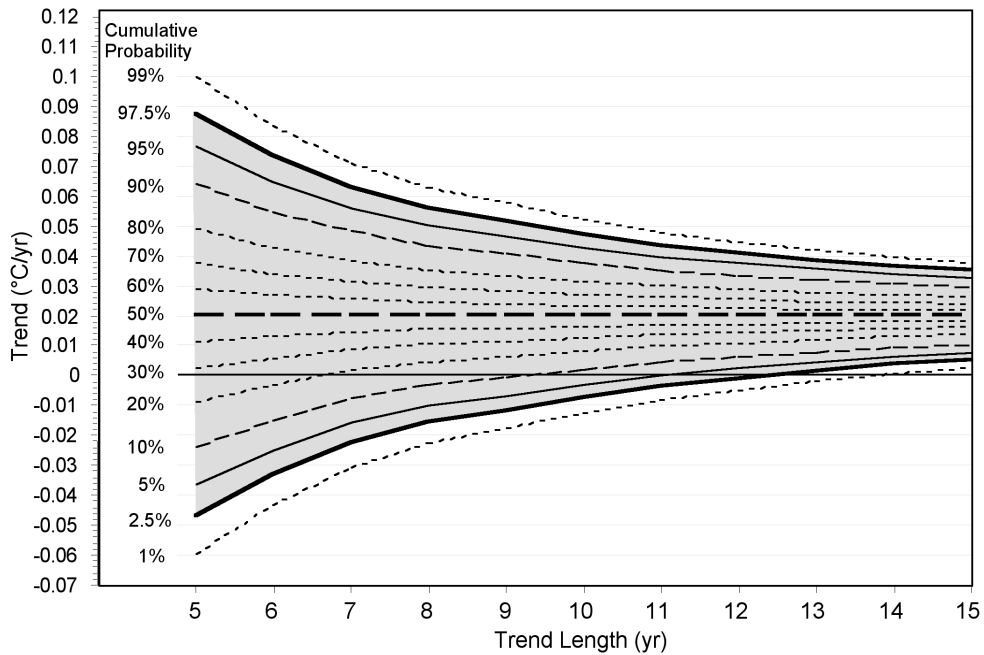
185

186

187 Auxiliary Figure 1.

188

189



190

191 Auxiliary Figure 1. Cumulative probability distribution of trend values for trends ranging  
192 in length from 5 to 15 years derived from 20 models under SRES A1B for the period  
193 January 2001 through December 2020 for global average MSU lower troposphere  
194 temperatures. The 95% confidence range is shaded in grey and a zero trend is indicated  
195 by the horizontal black line.

196

197